



# Geniposide augments apoptosis in fibroblast-like synoviocytes by restoring hypoxia-enhanced JNK-BNIP3-mediated autophagy

Deng Ran<sup>1,2</sup> · Wang Yan<sup>1,3,4</sup> · Bu Yanhong<sup>1,3,4</sup> · Wu Hong<sup>1,3,4</sup>

Received: 16 November 2022 / Revised: 6 July 2023 / Accepted: 7 August 2023 / Published online: 25 August 2023  
© The Author(s), under exclusive licence to Springer Nature Switzerland AG 2023

## Abstract

**Background** As the main effector cells of chronic inflammation and hyperplasia of synovium, fibroblast-like synoviocytes (FLSs) show abnormal proliferation and insufficient apoptosis in the hypoxic microenvironment, which is due to the increase of BNIP3-mediated autophagy. This study aimed to explore the mechanism of geniposide (GE) on hypoxia-induced hyperproliferative FLSs with a focus on autophagy and the JNK-BNIP3 pathway.

**Methods** The dynamic changes of autophagy, apoptosis, and hypoxia-related proteins in adjuvant arthritis (AA) rats were detected by immunohistochemistry and Western blot. The proliferation, autophagy, apoptosis, and mitochondrial state of FLSs were detected by CCK-8, flow cytometry, immunofluorescence, and transmission electron microscopy, respectively. Western blot, qRT-PCR, and co-immunoprecipitation were used to detect the expression of the JNK-BNIP3 pathway.

**Results** The excessive accumulation of BNIP3 in the synovium of AA rats was accompanied by inhibition of apoptosis and an increase in autophagy. GE inhibited the expression of BNIP3, enhanced apoptosis, decreased autophagy, and improved chronic inflammation and hyperplasia of synovium. The amount of autophagy under different oxygen concentrations was the key to mediating the different survival rates of FLSs, and the inhibition of autophagy triggered apoptosis. GE suppressed the proliferation of FLSs and down-regulated autophagy, leading to the accumulation of ROS and the decrease of mitochondrial membrane potential, induced the increase of apoptosis, and suppressed the accumulation of BNIP3 and the hyperphosphorylation of JNK.

**Conclusion** GE inhibited autophagy by restoring the hypoxia-induced activated JNK-BNIP3 pathway, inducing mitochondrial oxidative damage, augmented apoptosis, and decreased survival rate of FLSs.

**Keywords** Geniposide · JNK-BNIP3 pathway · Autophagy · Apoptosis · Fibroblast-like synoviocytes

## Introduction

Rheumatoid arthritis (RA) is an autoimmune disease characterized by chronic inflammation and the hyper-proliferation and invasiveness of synovial tissue [1]. Overactivation of fibroblast-like synoviocytes (FLSs), a major participant in synovial hyperplasia, is the central event of RA synovial hyperplasia. The abnormal proliferation and insufficient apoptosis of FLSs are consistent with the pathological features of synovial hyperplasia [2]. FLSs with active invasion characteristics are regarded as the "trigger point" in the progression of RA. Drugs that inhibit the changes in the properties of FLSs contribute to the control of synovial hyperplasia.

Hypoxia is an inherent feature of the synovial microenvironment, and its mediated synovial hyperplasia is one of the pathogenesis of RA. Hypoxia is a harsh microenvironment

---

Responsible Editor: John Di Battista.

✉ Wu Hong  
wuhongprof@aliyun.com

<sup>1</sup> Key Laboratory of Xin'an Medicine, Ministry of Education, Hefei 230012, China

<sup>2</sup> School of Integrated Chinese and Western Medicine, Anhui University of Chinese Medicine, Hefei 230012, China

<sup>3</sup> College of Pharmacy, Anhui University of Chinese Medicine, Qian Jiang Road 1, Hefei 230012, China

<sup>4</sup> Anhui Province Key Laboratory of Research & Development of Chinese Medicine, Hefei 230012, China

for normal cells. Autophagy is an important regulatory mechanism for cells to adapt to changes in the environment, which is crucial for cell survival, and abnormalities of autophagy are involved in a variety of diseases [3, 4]. Hyperactive autophagy has been confirmed in FLSs [5, 6]. The role of autophagy in cell death is twofold. On the one hand, increased autophagy made FLSs resistant to the trigger of apoptosis. On the other hand, suppression of the PI3K-AKT pathway up-regulated autophagy, which led to autophagic cell death and induced a decrease in the proliferation of FLSs [7]. Does autophagy promote survival or induce cell death in the anoxic microenvironment of RA synovium?

The Bcl-2/adenovirus E1B 19-kDa interacting protein 3 (BNIP3), the only atypical BH3 member of the Bcl-2 family, is directly regulated by hypoxia-inducible factor-1 $\alpha$  (HIF-1 $\alpha$ ) [8]. Earlier studies have found that BNIP3 induced a decrease in mitochondrial membrane potential (MMP) and apoptosis [9]. With the deepening of research, BNIP3 also plays an important role in autophagy [10]. Previous studies have confirmed that compared with FLSs extracted from patients with osteoarthritis, FLSs have the characteristics of less apoptosis and stronger proliferation ability, which is closely related to the increase of autophagy mediated by hypoxia-induced BNIP3 [11]. At present, there is still controversy and contradiction about the function of BNIP3 to promote survival or death, but BNIP3 has been widely concerned and recognized as an inducer of autophagy.

As an iridoid glycoside extracted from dried and ripe fruits of *Gardenia jasminoides* Ellis, geniposide (GE) inhibited the S1P-S1PR1/3 pathway, down-regulated the abnormal proliferation of FLSs and induced apoptosis [12–14]. What is more, GE lowered the hyperphosphorylation of c-Jun N-terminal kinase (JNK) in adjuvant arthritis (AA) rats to relieve inflammatory reactions of synovium [15].

Previous studies have confirmed that GE has anti-inflammatory effects, but the intervention of GE on autophagy of FLSs under hypoxia is unclear. The aims of this study were to clarify the role of autophagy in RA and determine the effect of GE on autophagy, and to verify that inhibition of JNK-BNIP3-mediated autophagy in RA is the key to the protective effect of GE.

## Materials and methods

### Animals and drug application

32 male Sprague Dawley (SD) rats weighing 160–200 g from the Experimental Animal Center of Anhui University of Chinese Medicine were randomly divided into 4 groups: control, 15-day AA (15 d), 25-day AA (25 d), and 35-day AA (35 d). 48 male SD rats were divided into 6 groups

( $n = 8$ ): control, model, GE (60 mg/kg), 3-Methyladenine (autophagy inhibitor, 3-MA, 15 mg/kg, MCE, New Jersey, USA), and rapamycin (autophagy activation, Rapa, 2 mg/kg, MCE, New Jersey, USA), dexamethasone (Dex, 2.5 mg/kg, Solarbio, China, Beijing). 0.1 mL of complete Freund's adjuvant (Sigma) was injected subcutaneously into the left hind paw of the rat to establish the AA model [16]. From 15 to 24 days, rats were injected intraperitoneally with 3-MA (15 mg/kg), Rapa (2 mg/kg), and Dex (2.5 mg/kg), while GE (60 mg/kg) was gavage [17]. Synoviums were collected as experimental specimens for subsequent experiments.

All animal experiments were carried out with the approval of the Animal Care and Use Committee of the Anhui University of Chinese Medicine (AHUCM-rats-2021049).

### Histology and immunohistochemistry

Synovium was immediately fixed with 4% paraformaldehyde for 48 h and then dehydrated in 80%, 90%, 95%, and 100% ethanol for 2 h, respectively. The paraffin was immersed in the tissue for embedding, and synovium was sectioned laterally (4  $\mu$ m). Sections were stained with Hematoxylin and Eosin (H&E) and films were taken under a microscope to analyze the degree of synovial lesions.

Sample sections were dewaxed in xylene, hydrated in ethanol, then washed, and soaked in 3% H<sub>2</sub>O<sub>2</sub> to remove endogenous catalase. Slices were then boiled in the microwave for 3 min in citrate buffer. Sections for immunohistochemistry were incubated with antibodies against VCAM-1, Beclin-1, LC-3, BNIP3, HIF-1 $\alpha$ , Bcl-XL, and Bax diluted in TBS buffer (1:100) overnight at 4 °C and then incubated with goat anti-rabbit IgG (1:200) at 37 °C for 30 min. Finally, 3,3'-diaminobenzidine-stained sections were stained with hematoxylin for 0.5 min. Cells with brown nuclei were positive for protein expression.

### Cell culture and treatment protocols

FLSs, a cell line isolated from the synovium of patients with RA, were purchased from BeNa Culture Collection (Suzhou, China). FLSs were inoculated in Dulbecco's modified eagle medium (HyClone, New Zealand) containing 10% (v/v) fetal bovine serum (Biological Industries, Israel), 1% (v/v) 100 U/mL penicillin and 100 LG/mL streptomycin (Beyotime, Shanghai, China). Cells were cultured at 37 °C with 5% CO<sub>2</sub>. 0.5%, 2%, and 21% O<sub>2</sub> were used to treat FLSs to observe its survival state. After treatment with GE (100  $\mu$ M) [17], 3-MA (3 mM) [18], and RAPA (20 nM), FLSs were exposed to 2% O<sub>2</sub>, 93% N<sub>2</sub>, and 5% CO<sub>2</sub> in a hypoxic chamber (AIPUINS, USA) for 24 h [19].

### Cell viability assay

The Cell Counting Kit-8 (CCK-8) method was used to quantify cell viability according to the manufacturer's instructions. Optical density (OD) at 450 nm was measured on a microplate reader (SpectraMax iD3, USA).

### Cell proliferation assay

Cell proliferation was determined by 5-bromo-2'-deoxyuridine (BrdU) assay kit (Ribio, Guangzhou) according to the manufacturer's instructions. FLSs were exposed to 50 mM BrdU, incubated at 37 °C for 1.5 h, fixed with 4% formaldehyde for 15 min, and treated with 0.5% Triton X-100 for 20 min to increase permeability. Cells were treated with 100 µL of 16-Apollo reaction cocktail for 30 min. Nucleus was stained with 100 µL Hoechst 33,342 (5 mg/mL) for 10 min, and the films were observed under a fluorescence microscope.

### Cell cycle analysis

The pretreated FLSs were digested, centrifuged, and washed with 2 mL precooled PBS for 3 times and then fixed overnight with 75% precooled alcohol at 4 °C. FLSs were rinsed and resuspended in 500 µL PBS. 100 µL RNase (100 µg/mL) and 400 µL propidium iodide (PI, 50 µg/mL) were added, incubated in the dark for 30 min, and then filtered with 100 mesh nylon net. Before analysis, the samples were stored at 4 °C away from light and detected by flow cytometry at a wavelength of 488 nm within 1 h.

### Reactive oxygen species (ROS) measurement

DCFH-DA probe kit (Beyotime, Shanghai) was used to detect intracellular ROS content. FLSs were spread into a 35 mm culture dish at the density of  $1 \times 10^6$  and subjected to hypoxia. DCFH-DA probe molecules were diluted to the final concentration of 10 µM with serum-free medium and cultured in the dark at 37 °C for 20 min. After washing, FLSs were collected and measured by flow cytometry.

### Mitochondrial membrane potential (MMP) polychromatic assay

MMP was measured with cationic JC-1 (5,5',6,6'-tetrachloro-1,1',3,3'-tetraethyl benzimidazolylcarbocyanine iodine) dye. FLSs precipitates were collected and stained with 1 mL JC-1 staining working solution (Solarbio, Beijing) incubated at 37 °C for 20 min, and then washed twice with JC-1 staining buffer (1×). Samples were examined by flow cytometry.

### Apoptosis assay

Annexin V-FITC/PI double staining kit was used to detect apoptosis (Bestbio, Shanghai). FLSs precipitates were collected and washed twice with PBS, then resuspended with 400 µL of 1× Annexin V binding solution. 10 µL FITC-labeled Annexin-V were added to FLSs suspension and incubated in the dark for 20 min. 5 µL of PI staining solution was added and incubated at 4 °C for 5 min in the dark. The number of positive staining was detected by flow cytometry within 1 h.

### TUNEL assay

The TdT-mediated dUTP Nick End Labeling (TUNEL) method was used to label apoptotic cells. Immunofluorescence double staining was performed according to the manufacturer's instructions (Servicebio, Wuhan). The nuclei were stained with DAPI and the images were observed under a fluorescence microscope. The apoptotic cells were green and the nuclei were blue.

### Transmission electron microscope

FLSs were digested and centrifuged to collect precipitates, fixed with 2.5% glutaraldehyde for 24 h, washed with PBS and then fixed with 1% staining acid for 2 h. FLSs were placed at 50%, 75%, and 90% gradient concentrations of ethanol, 90% ethanol-90% acetone, 90% acetone, and 100% acetone for 20 min, respectively, to remove water. Cells were embedded in pure acetone and embedding solution in a volume of 2:1 for 3 h and then cured in an oven at 60 °C for 24 h. After sectioning with an ultra-thin slicer, FLSs were stained with 3% uranyl acetate-lead citrate double staining, and the films were visualized under a transmission electron microscope.

### Laser-scanning confocal microscopy

FLSs were transfected with green fluorescence protein microtubule-associated protein 1 light chain 3B (EGFP-LC3B) plasmid (Genomeditech, Shanghai) to specifically label autophagosomes. Mito-tracker red (a special mitochondrial marker, Beyotime, Shanghai) with a concentration of 100 nM was incubated at 37 °C for 30 min, then treated with DAPI for 5 min (10 µg/mL, Biosharp, China). 1 mL of 4% paraformaldehyde was added to FLSs after hypoxia at room temperature for 30 min. After washing with PBS, 1 mL of 0.1% Triton-X 100 was added to the cells at room temperature for 15 min. Then the cells were prepared, and observed with a confocal laser scanning microscope (ZEISS, Oberkochen, Germany).

## Western blot

Proteins were extracted from FLSs (synovium) and lysed with RIPA buffer (Beyotime, Shanghai) containing 1% (v/v) protease inhibitor. The extracted proteins were separated by 12% sodium dodecyl sulfate–polyacrylamide gel electrophoresis (SDS-PAGE) and transferred to NC membranes. Western blot was performed as previously described [16]. We examined the expressions of HIF-1 $\alpha$ , BNIP3, LC3, Beclin-1, PINK1, Bax, Bcl-XL, and  $\beta$ -actin (1:1000). The gel images were obtained with ECL reagent (Biosharp, China), and results were normalized to  $\beta$ -actin. The intensity of bands was quantified with AlphaView SA software.

## qRT-PCR analysis

qRT-PCR analysis was performed according to our previous study [16]. Primers for polymerase chain reaction were as follows: HIF-1 $\alpha$ , forward, 5'-TTCCCGACT AGGCC ATTC-3' and reverse, 5'-CAGGTATTCAAGGTCCCA TTTCA-3'; BNIP3, forward, TCCAGCCTCGGTTTC TATTT and reverse, AGCTCTTGGAGCTACTCCGT, GAPDH, forward, GCGGGAAATCGTGCGTGAC and reverse, CGTCATACTCCTGCTTGCTG. SYBR Green (Bimake, America) was used to quantify gene expression. The mRNA level of each independently prepared RNA was determined by qRT-PCR in triplicate and normalized to the GAPDH level.

## Co-immunoprecipitation (Co-IP)

FLSs were seeded in 100 mm petri dishes, and 1 mL IP lysate containing cocktail inhibitor was added to it and incubated on ice for 30 min. Cells were lysed and centrifuged at 14,000 rpm for 10 min. The cell lysate was collected, and equivalent protein, 2  $\mu$ g mouse IgG, and 40  $\mu$ L Protein A/G beads were incubated at 4  $^{\circ}$ C for 4 h to remove the non-specific binding. After centrifugation (3500 rpm, 5 min), supernatant and 2  $\mu$ g anti-Flag antibody and 40  $\mu$ L protein A/G beads were incubated overnight at 4  $^{\circ}$ C. To isolate immunoprecipitated complexes, the precipitation was washed with IP lysate for 5 times and centrifuged at 3500 rpm for 5 min. 2 $\times$ Laemmli buffer and precipitation complex were shaken and mixed evenly, boiled for 10 min and centrifuged (12,000 rpm, 5 min), and the supernatant was transferred to 4  $^{\circ}$ C. Finally, Western blot was used to detect the target protein.

## Statistical analysis

T-test and repeated measures two-way ANOVA test were used to analyze the data with SPSS 22.0. The value of  $P < 0.05$  was considered statistically significant.

## Results

### Dynamic changes in autophagy and apoptosis in synovium of AA rats

H&E staining showed that the synovium of AA rats was abnormally thickened and accompanied by infiltration of inflammatory cells in the synovium stroma. With the prolongation of modeling time, the degree of synovium hyperplasia intensified (Fig. 1A). Moreover, immunohistochemical staining showed that the expression of VCAM-1, a surface marker of FLSs, was also increased (Fig. 1B), and the expressions of autophagy associated proteins (LC3 and Beclin-1) increased in synovium with the extension of modeling time (Fig. 1C). In terms of the occurrence of apoptosis, the expression of pro-apoptotic protein Bax was observed in normal synovium, but decreased in a time-dependent manner, and anti-apoptotic protein Bcl-XL showed the opposite trend (Fig. 1D). Western blotting again confirmed the dynamic changes in autophagy and apoptosis in the synovium (Fig. 1F, G). These results indicated that cell death occurred through a combination of autophagy and apoptosis in the synovium of AA rats, and with the extension of modeling time, autophagy enhanced but apoptosis was inhibited, which was accompanied by the accumulation of hypoxia-related protein (HIF-1 $\alpha$  and BNIP3) (Fig. 1E, H). The synovium was in a state of hypoxia, and the degree of hypoxia was further aggravated with the extension of time.

### Effects of different oxygen concentrations on FLSs survival

The activity of FLSs increased with the decrease of oxygen concentration, and its proliferative activity decreased when oxygen concentration was below 2% (Fig. 2A). Therefore, FLSs treated with 2% O<sub>2</sub> for 24 h were considered as moderate hypoxia, and 0.5% O<sub>2</sub> for 24 h was defined as severe hypoxia. The survival status was evaluated from the aspects of proliferation, autophagy, apoptosis, and mitochondrial redox status. The results of BrdU incorporation showed that the proliferation capacity of FLSs increased significantly at 2% O<sub>2</sub>, but decreased at 0.5% O<sub>2</sub> (Fig. 2B). The apoptosis rate of FLSs was lower at 21% and 2% O<sub>2</sub>

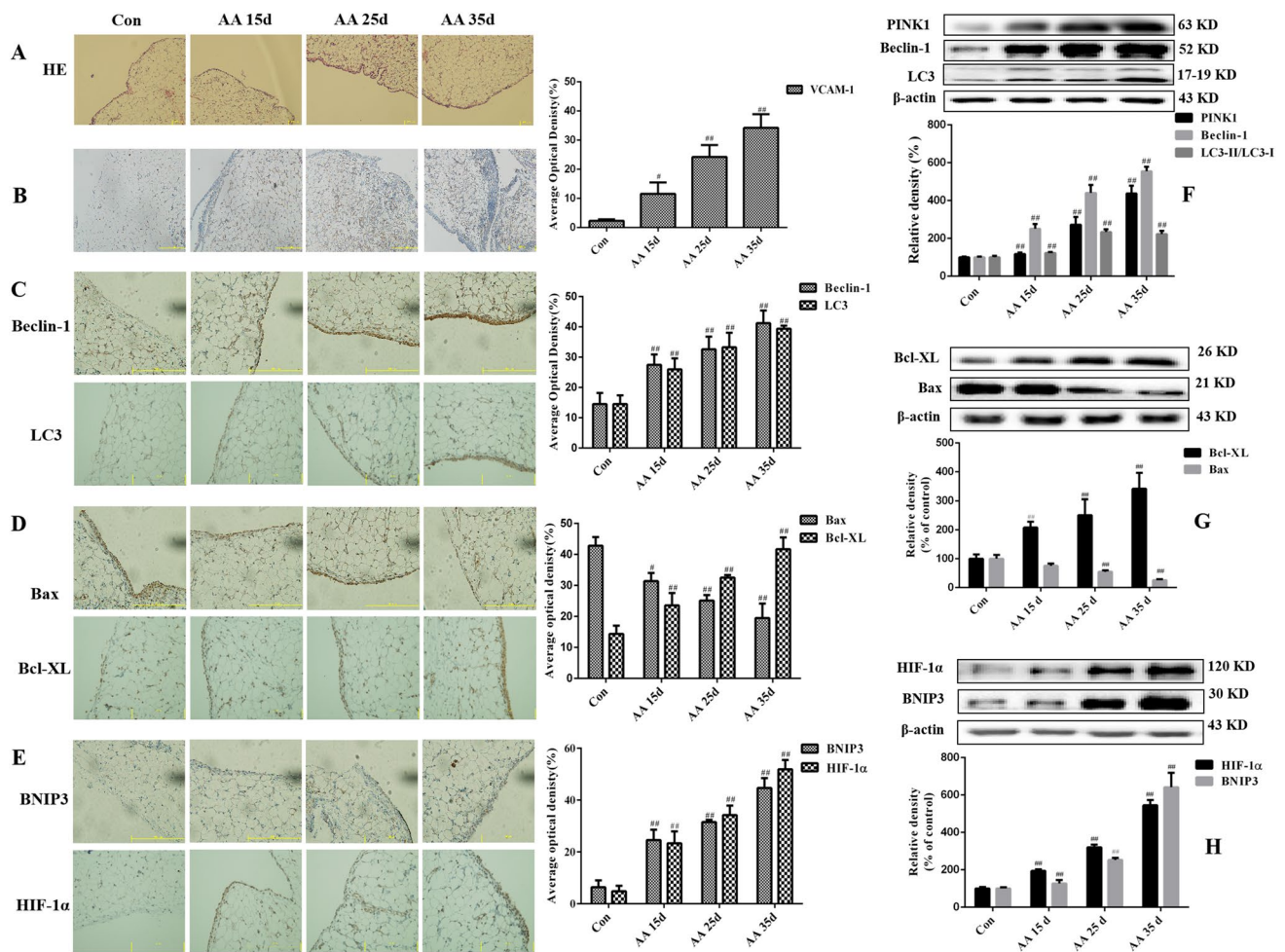


**Fig. 1** Dynamic changes of autophagy and apoptosis in joint synovium at different stages in AA rat model. **A** H&E staining for synovium of AA rats at different stages; **B–E** Immunohistochemical staining for VCAM-1 (**B**), Beclin-1 and LC3 (**C**), Bax and Bcl-XL (**D**), BNIP3 and HIF-1α (**E**); **F–H** Western blotting for autophagy

protein expressions (**F**), apoptosis protein expressions (**G**) and hypoxia-related protein expressions (**H**). Values were expressed as the mean  $\pm$  SD,  $n=6$ . # $P<0.05$ , ## $P<0.01$  compared with control group; \* $P<0.05$ , \*\* $P<0.01$  compared with model group

( $5.13\% \pm 0.78\%$ ,  $4.15\% \pm 0.26\%$ ) and increased at  $0.5\% O_2$  ( $14.65\% \pm 0.86\%$ ) (Fig. 2C, D). ROS produced during oxidative stress is directly involved in the regulation of cell survival and death. The decline of mitochondrial membrane potential is a landmark event in the early stage of apoptosis. Flow cytometry was used to detect intracellular ROS content and MMP changes. Compared with  $21\% O_2$ , there was only a slight increase in ROS accumulation and MMP reduction in FLSs at  $2\% O_2$ , while ROS increased significantly and MMP decreased at  $0.5\% O_2$  (Fig. 2E–G). The stability of ROS and MMP at  $2\% O_2$  confirmed that the redox state was in equilibrium and apoptosis did not occur in FLSs. At  $0.5\% O_2$ , the accumulation of ROS led to redox imbalance, inducing a decrease in MMP and cell apoptosis, which was

the main factor for the significant reduction of FLSs survival rate caused by  $0.5\% O_2$ .

The currently widely used autophagy detection method is to observe EGFP-LC3 fluorescent spots. The green fluorescent EGFP within the cell represents autophagosomes, while the living dye Mito-Tracker Red dyes mitochondria with red fluorescence. The overlap of red and green fluorescence represents the occurrence of autophagy. The dispersion or spot-like aggregation of EGFP fluorescence can accurately reflect the cell state. In the physiological environment, LC3 is distributed in a diffuse manner. When autophagy is activated, LC3 transfers to autophagic vesicles, and EGFP-LC3 was significantly granulated in FLSs at  $2\% O_2$ , which was one of the classic features of autophagy. The shape of mitotracker-labeled

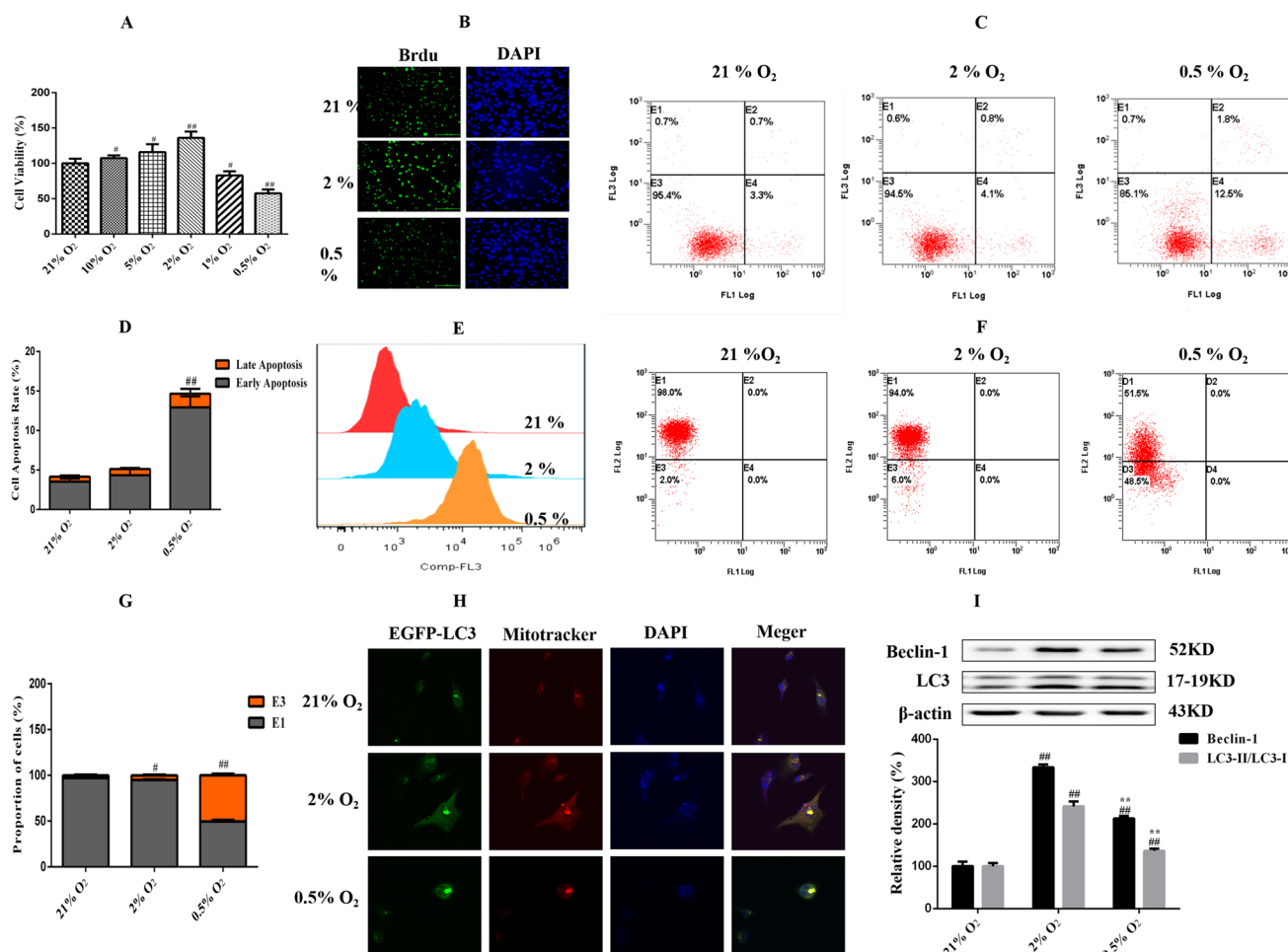


**Fig. 2** Effects of different oxygen concentrations on cell survival and autophagy. **A** The effects of different oxygen concentrations on the viability of FLSs were detected by CCK-8 method; **B** BrdU was incorporated into FLSs, FLSs were exposed to 21%, 2% or 0.5% O<sub>2</sub> for 24 h, and then cells were stained with BrdU (green) and propidium iodide (blue). **C** after exposed to different oxygen concentrations, FLSs were analyzed by flowcytometry using AV/PI double-staining; **D** histogram depicts the quantitative data from the AV/PI double-staining; **E** FLSs were assessed the ROS content

by flowcytometry; **F** JC-1 was used to detect the effect of hypoxia on MMP of FLSs; **G** histogram depicts the quantitative data from the JC-1 staining; **H** FLSs were infected with EGFP-LC3 (Green) for 24 h and then exposed to different oxygen concentrations, mitochondria were marked with Mitotracker (Red); nuclei were stained with DAPI (blue). **I** The expressions of Beclin-1 and LC3 were analyzed by Western blot. Values were expressed as the mean  $\pm$  SD,  $n=3$  for each group.  $^{\#}P<0.05$ ,  $^{\#\#}P<0.01$  compared with 21% O<sub>2</sub>,  $^*P<0.05$ ,  $^{**}P<0.01$  compared with 2% O<sub>2</sub> (color figure online)

mitochondria did not change significantly, but the colocalization of EGFP-LC3 and mitotracker increased. At 0.5% O<sub>2</sub>, FLSs were circular; mitotracker-labeled mitochondria were unevenly distributed and showed different aggregation states from 21%, 2% O<sub>2</sub> (Fig. 2H). Western blotting again confirmed that although autophagy was also induced under 0.5% O<sub>2</sub>, it was less than that under 2% O<sub>2</sub> (Fig. 2I).

### Effect of intervention autophagy on apoptosis in synovium of AA rats

The effect of autophagy on apoptosis in synovium was investigated by autophagy inhibitor 3-MA and autophagy activator Rapa. 3-MA (15 mg/kg) and Dex (2.5 mg/kg) alleviated synovial hyperplasia and inflammatory infiltration (Fig. 3A). Similarly, 3-MA and Dex induced the decrease of VCAM-1 and autophagy associated proteins (LC3-II/LC3-I ratio, Beclin-1, and PINK1) in the synovium (Fig. 3B, C, F). Anti-apoptotic protein (Bcl-XL), hypoxia-related protein (HIF-1 $\alpha$  and BNIP3) were decreased, while pro-apoptotic protein (Bax) increased (Fig. 3D, E, G, H). Taken together, suppression of autophagy induced increased apoptosis in the

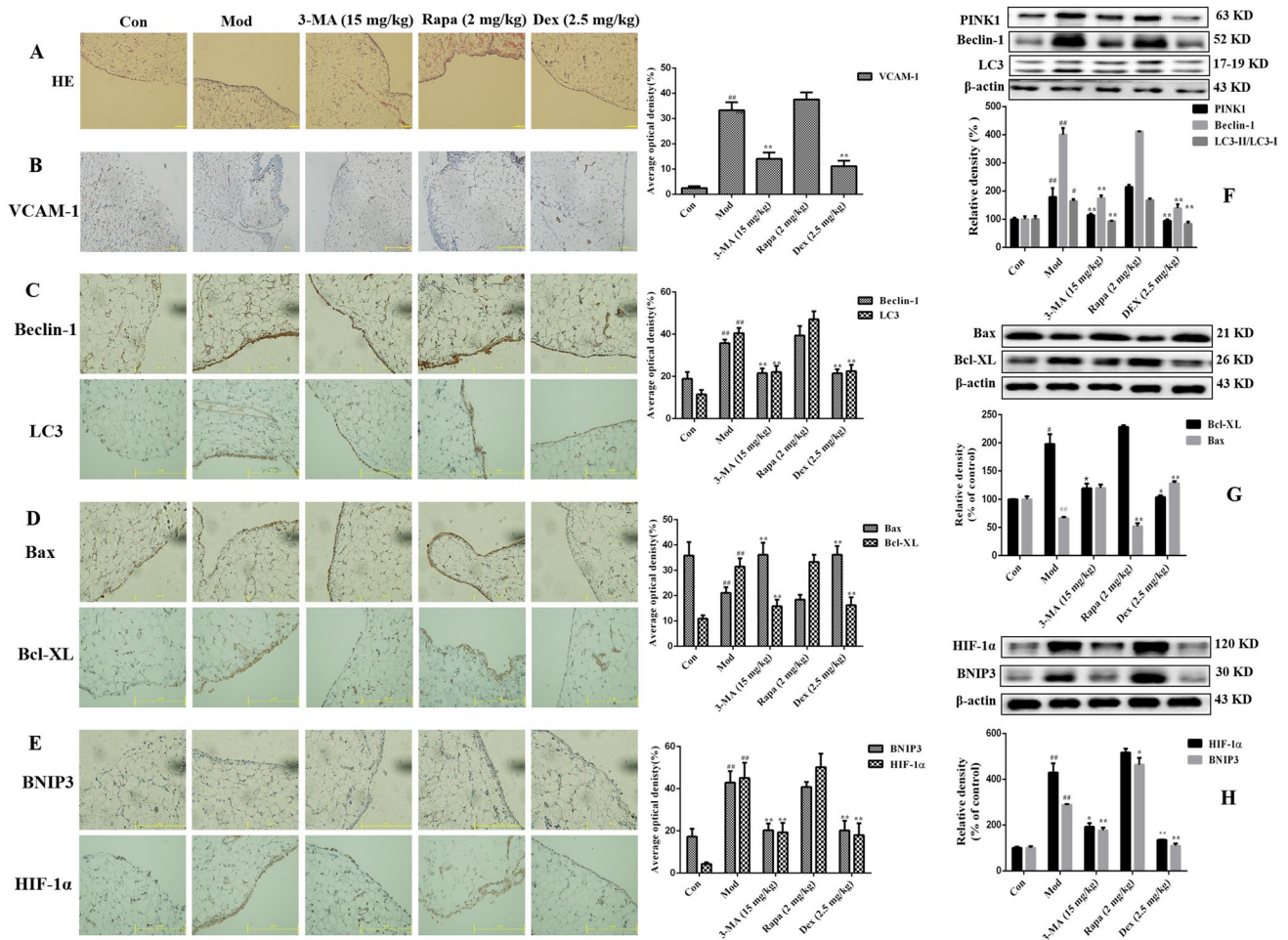


**Fig. 3** Changes of apoptosis in synovium of AA rats after inhibiting or promoting autophagy. **A** H&E staining for synovium of AA rats; **B–E** Immunohistochemical staining for VCAM-1 (**B**), Beclin-1 and LC3 (**C**), Bax and Bcl-XL (**D**), BNIP3 and HIF-1 $\alpha$  (**E**); **F–H** Western blotting for autophagy protein expressions (**F**), apoptosis protein

expressions (**G**) and hypoxia-related protein expressions (**H**). Values were expressed as the mean  $\pm$  SD,  $n=6$ . # $P < 0.05$ , ## $P < 0.01$  compared with control group; \* $P < 0.05$ , \*\* $P < 0.01$  compared with model group

synovium, accompanied by an improvement in the hypoxic microenvironment.

Rapa (2 mg/kg) aggravated synovial hyperplasia and joint injury (Fig. 3A), inhibited apoptosis (Fig. 3D, G) by activating autophagy (Fig. 3B, E) in synovium, which was accompanied by intensification of hypoxia (Fig. 3E, H).

### Suppression of autophagy on the survival of FLSs

To clarify the regulation of autophagy on the survival state, FLSs were treated with 3-MA (3 mM), and the changes in proliferation, apoptosis, and mitochondrial redox state were observed. 3-MA (3 mM) suppressed autophagy (Fig. 4A, B) and cell survival rate at 21%, 2%, and 0.5% O<sub>2</sub> (Fig. 4C, D). Under 21% O<sub>2</sub>, the apoptosis rate of FLSs did not change significantly after 3-MA treatment ( $5.96\% \pm 0.94\%$  vs  $4.7\% \pm 0.44\%$ ), while significantly enhanced under

2% and 0.5% O<sub>2</sub> ( $15.37\% \pm 0.33\%$  vs  $5.47\% \pm 0.35\%$ ;  $24.03\% \pm 1.39\%$  vs  $15.30\% \pm 1.40\%$ ) (Fig. 4E, F). At 2% O<sub>2</sub>, apoptosis was obviously triggered when autophagy was suppressed, while apoptosis was slightly increased, but to a lesser extent under 0.5% O<sub>2</sub>.

MA (3 mM) had no significant effect on ROS and MMP, indicating that the occurrence of autophagy was small at 21% O<sub>2</sub>. The accumulation of ROS and the decreased proportion of MMP in FLSs increased significantly at 2% O<sub>2</sub> due to the inhibition of autophagy by 3-MA. Under 0.5% O<sub>2</sub>, the accumulation of ROS and the proportion of MMP reduction increased further (Fig. 4G-I).

Altogether, at 2% O<sub>2</sub>, inhibition of autophagy induced an increase in apoptosis, while apoptosis also increased to a certain extent after inhibition of autophagy under 0.5% O<sub>2</sub>. Combined with the results of autophagy, it can be inferred that FLSs still have a certain amount of autophagy under

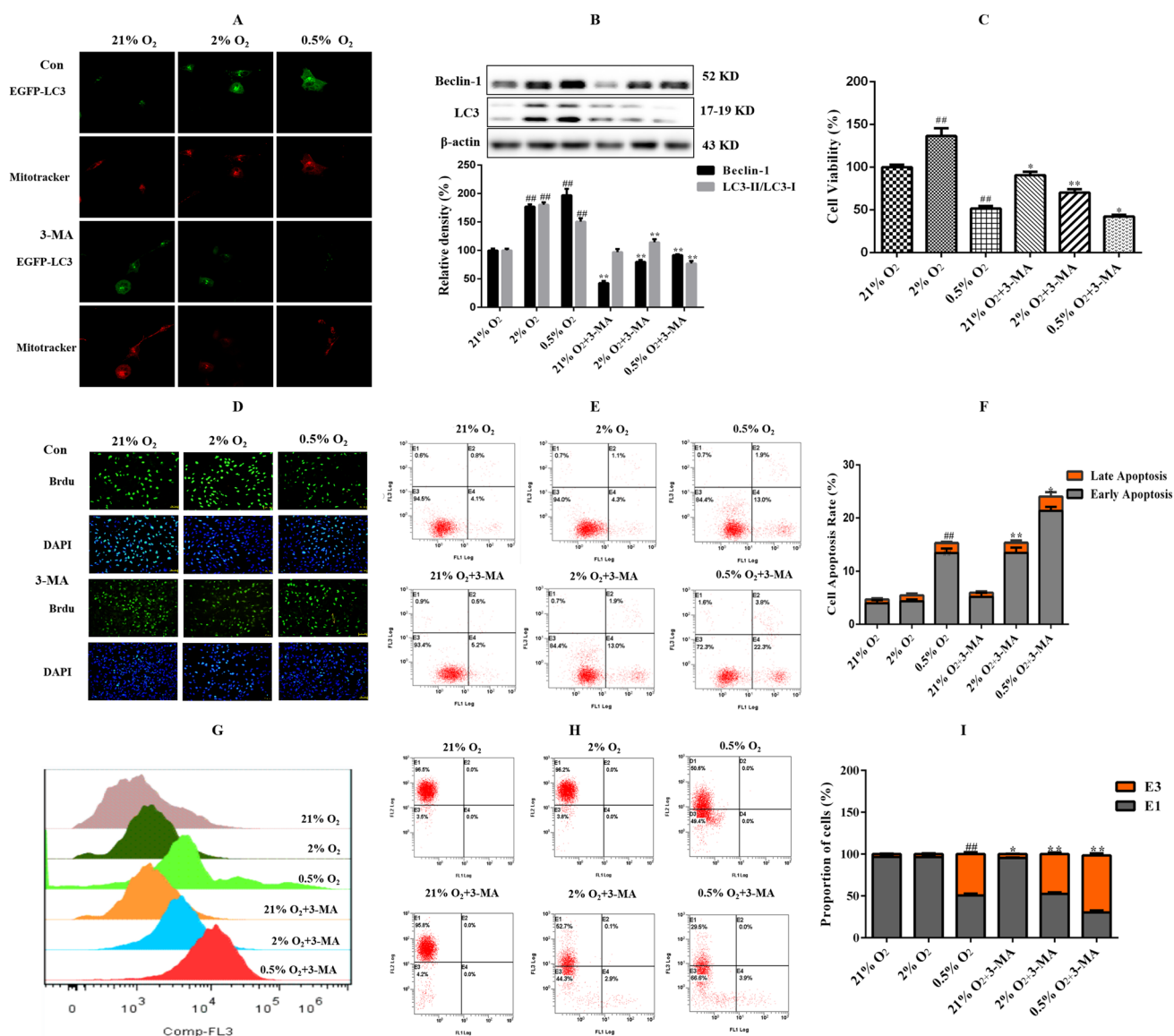


**Fig. 4** Effects of inhibition of autophagy by 3-MA on the survival of FLSs. **A** FLSs were treated with 3-MA (3 mM) and then exposed to different oxygen concentrations for 24 h. Cell viability was measured by CCK-8 assay; **B** FLSs were stained with BrdU (green) and propidium iodide (blue). **C** FLSs were analyzed by flowcytometry using AV/PI double-staining; **D** Histogram depicts the quantitative data from the AV/PI double-staining; **E** FLSs were assessed the ROS content by flowcytometry; **F** JC-1 was used to detect the effect of 3-MA under 21%, 2% or 0.5% O<sub>2</sub> on MMP of FLSs; **G** Histogram depicts

the quantitative data from the JC-1 staining; **H** FLSs were infected with EGFP-LC3 (Green) for 24 h and then treated with 3-MA, mitochondria were marked with Mitotracker (Red). **I** The expressions of Beclin-1 and LC3 were analyzed by Western blot. Values were expressed as the mean  $\pm$  SD. Statistical analysis were shown three independent replicates. <sup>#</sup> $P < 0.05$ , <sup>##</sup> $P < 0.01$  compared with 21% O<sub>2</sub>; <sup>\*</sup> $P < 0.05$ , <sup>\*\*</sup> $P < 0.01$  compared with 21% O<sub>2</sub> + 3-MA, 2% O<sub>2</sub> + 3-MA or 0.5% O<sub>2</sub> + 3-MA (color figure online)

0.5% O<sub>2</sub>, but it was not enough to eliminate the excessive accumulation of ROS and the decrease of MMP caused by severe hypoxia at 0.5% O<sub>2</sub> and induced the increase of apoptosis and the decline of cell survival rate.

### Inhibition of autophagy by GE enhanced apoptosis in synovium of AA rats

GE (60 mg/kg) significantly alleviated the abnormal hyperplasia and inflammatory infiltration of the synovium (Fig. 5A). GE (60 mg/kg) decreased VCAM-1 expression and autophagy-associated proteins (LC3-II/LC3-I ratio, Beclin-1, and PINK1) (Fig. 5B, C, F), while anti-apoptotic protein (Bcl-XL)



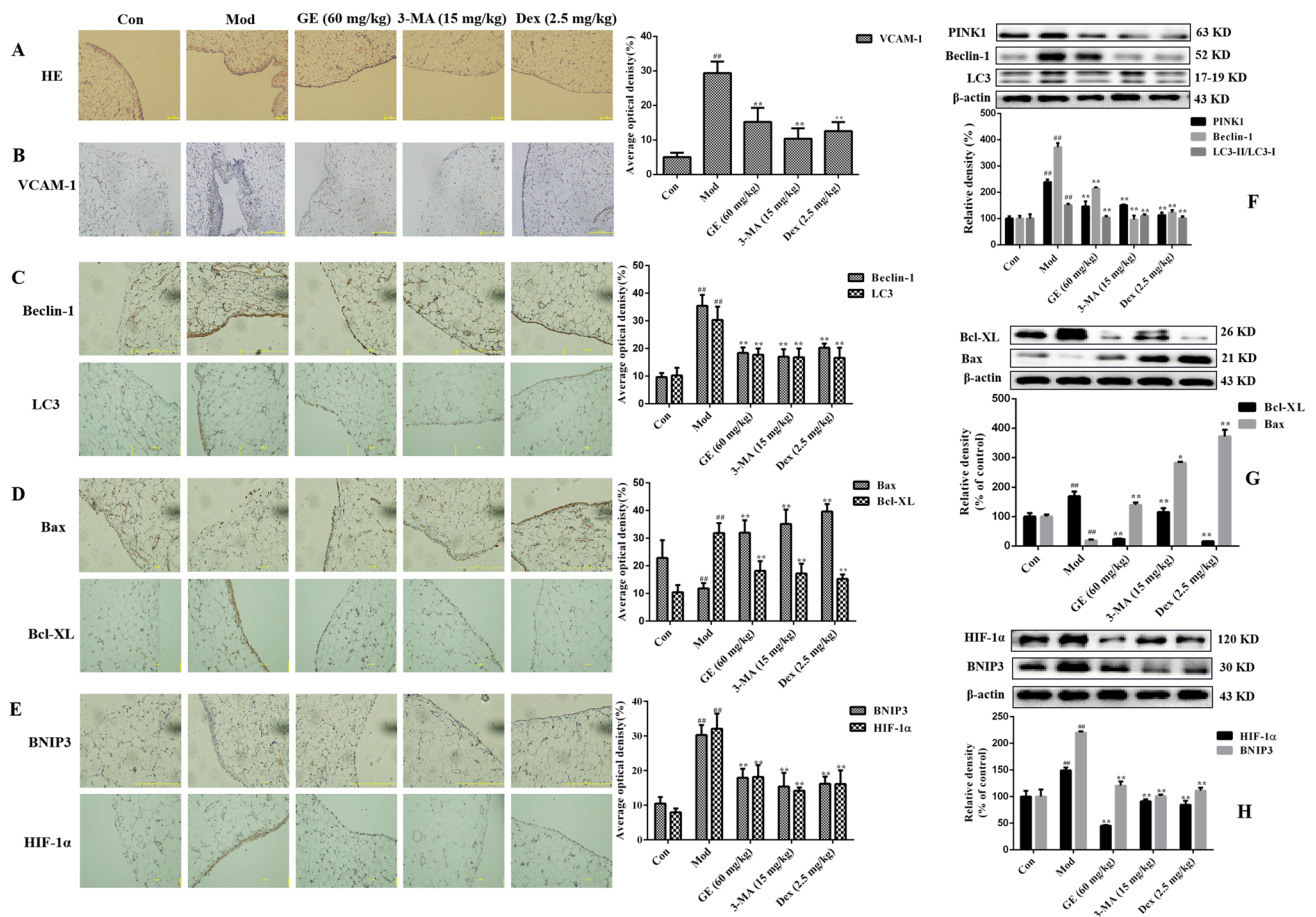


**Fig. 5** Effects of GE on autophagy and apoptosis in synovium of AA rats. **A** H&E staining for synovium of AA rats; **B–E** Immunohistochemical staining for VCAM-1 (**B**), Beclin-1 and LC3 (**C**), Bax and Bcl-XL (**D**), BNIP3 and HIF-1 $\alpha$  (**E**); **F–H** western blotting for

autophagy protein expressions (**F**), apoptosis protein expressions (**G**) and hypoxia-related protein expressions (**H**). Values were expressed as the mean  $\pm$  SD,  $n = 6$ .  $^{\#}P < 0.05$ ,  $^{\#\#}P < 0.01$  compared with control group;  $^*P < 0.05$ ,  $^{**}P < 0.01$  compared with model group

decreased and pro-apoptotic protein (Bax) increased (Fig. 5D, G). Meanwhile, hypoxia-related protein (HIF-1 $\alpha$  and BNIP3) decreased with the improvement of synovial hyperplasia (Fig. 5E, H). Taken together, GE inhibited autophagy and promoted apoptosis to improve synovial dysplasia and hypoxic microenvironment in AA rats.

### GE suppressed the hypoxia-induced proliferation in FLSs

In vivo experiments have confirmed that the synovium of AA rats was in the hypoxic microenvironment. Previous research has confirmed that FLSs had the strongest proliferation ability at 2% O<sub>2</sub>, and it is the most suitable concentration for establishing an in vitro hypoxia model of FLSs [11]. GE (100  $\mu$ M) had the most significant inhibitory effect (Fig. 6A), and it was selected in the subsequent experiments [17]. PI was used to determine the effect of GE on the cell cycle and proliferation index of FLSs. At 21% O<sub>2</sub>, the G2/M phase proportion

was 8.51%  $\pm$  0.89%; the proportion of G2/M phase induced by 2% O<sub>2</sub> increased to 23.21%  $\pm$  5.51%, while GE (100  $\mu$ M) decreased it to 10.44%  $\pm$  0.35% (Fig. 6B, C). BrdU incorporation method was consistent with the results of PI. After GE (100  $\mu$ M) administration, the fluorescence intensity of BrdU in FLSs decreased significantly (Fig. 6D). CCK-8 assay also showed that GE reduced the cell viability of FLSs under hypoxia (Fig. 6E).

### GE reduced hypoxia-enhanced autophagy and augmented apoptosis

The results of the electron microscope showed that the nuclear membrane of FLSs was intact, cytoplasmic vacuoles were less at 21% O<sub>2</sub>, and the oval bilayer membrane and cristae of mitochondria were clear. At 2% O<sub>2</sub>, the nuclear membrane of FLSs was smooth, and a large number of mitochondria were dumbbell shaped, but an increase of vacuoles covering or contacting mitochondria was observed. After

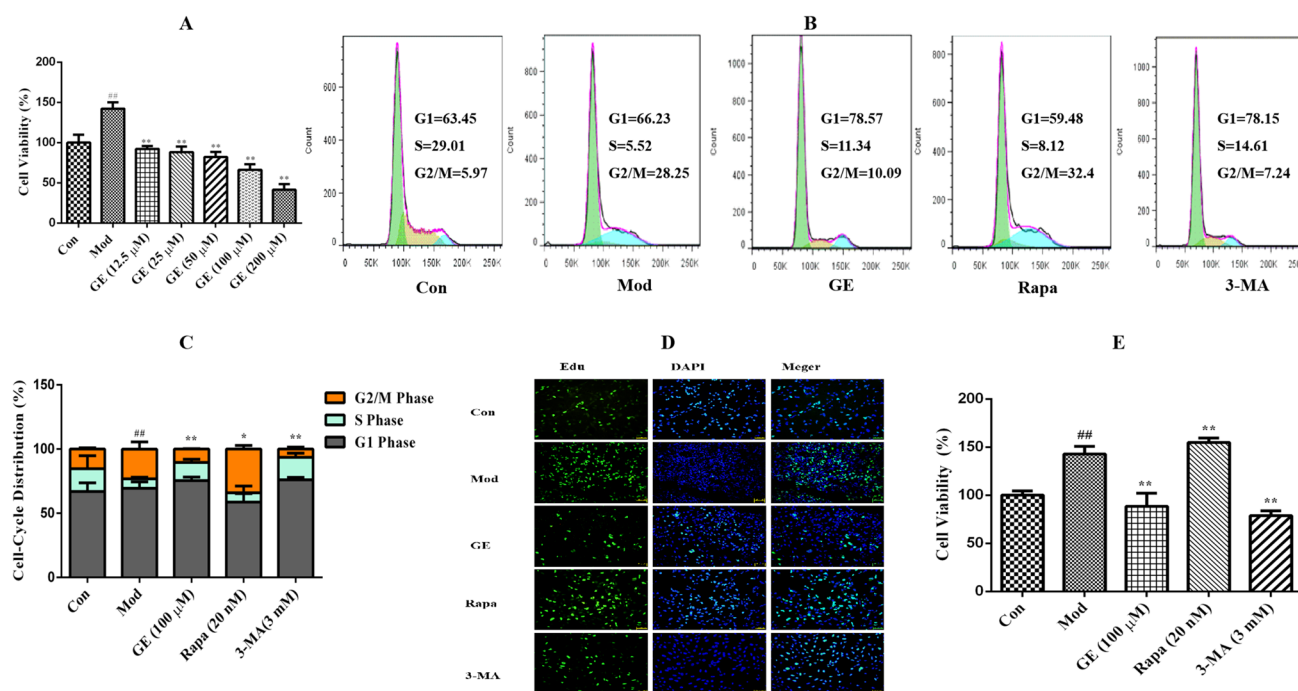


**Fig. 6** Effects of GE on the proliferation of FLSs. **A** The effects of different GE concentrations on the viability of FLSs were detected by CCK-8 method; **B** Flowcytometry analyzed the cell proliferation with PI staining after FLSs were treated with GE; **C** Histogram depicts quantitative data from the flow cytometric analysis; **D** BrdU was incorporated into FLSs, and then BrdU (green) and DAPI (blue)

immunostaining were detected; **E** The effect of GE on the activity of FLSs was detected by CCK-8 method. Values were expressed as the mean  $\pm$  SD. Statistical analysis were shown three independent replicates.  $\#P < 0.05$ ,  $\#\#P < 0.01$  compared with control group;  $*P < 0.05$ ,  $**P < 0.01$  compared with model group (color figure online)

treatment with Rapa (20 nM), the incidence of autophagy in FLSs further increased, but an intact mitochondrial structure was observed. After treatment with GE (100  $\mu$ M) and 3-MA (3 mM), the nuclear membrane of FLSs showed irregular crimp and vacuoles increased. Although many mitochondria still maintained the bilayer structure, their contents and crest structures almost disappeared, indicating that the normal structure of mitochondria was seriously damaged, and the crest structure and matrix of executive function disappeared (Fig. 7A). Fluorescence co-localization results showed that 2%  $O_2$  induced the formation of EGFP-LC3 puncta, while Rapa (20 nM) further increased it, while GE (100  $\mu$ M) and 3-MA (3 mM) inhibited these phenomena (Fig. 7B). The ratio of LC3-II/LC3-I and Beclin-1 increased at 2%  $O_2$ . GE (100  $\mu$ M) and 3-MA (3 mM) reduced LC3-II/LC3-I and Beclin-1 significantly, while Rapa (20 nM) increased it (Fig. 7C). The important reason why FLSs maintain abnormal proliferation at 2%  $O_2$  was the high level of autophagy [11], while GE inhibited autophagy, resulting in a significant decline in cell survival.

The effect of GE on the apoptosis of FLSs was further investigated. The apoptosis rate of FLSs was low at 21% and 2%  $O_2$  ( $4.13\% \pm 0.82\%$ ,  $5.33\% \pm 0.36\%$ ), while

increased ( $14.40\% \pm 1.46\%$ ) after GE (100  $\mu$ M) treatment (Fig. 8A, B). TUNEL staining and the expressions of apoptosis-associated proteins (Bax and Bcl-XL) further confirmed that GE (100  $\mu$ M) induced apoptosis (Fig. 8C, D). At 2%  $O_2$ , 3-MA (3 mM) increased the apoptosis rate of FLSs ( $25.20\% \pm 1.56\%$ ), while decreased after Rapa (20 nM) treatment ( $1.05\% \pm 0.44\%$ ), which confirmed that inhibition of hypoxia-induced autophagy triggered apoptosis.

### GE-induced redox imbalance in FLSs

After treatment with 21% and 2%  $O_2$ , FLSs were incubated with fluorescent ROS and JC-1 molecular probes. There was no significant change in ROS and MMP in FLSs at 2%  $O_2$ , but GE (100  $\mu$ M) and 3-MA (3 mM) induced ROS accumulation and the proportion of FLSs with decreased MMP increased, while Rapa (20 nM) had no significant effect on ROS and MMP (Fig. 9A–C).

Combined with the results of autophagy and apoptosis, it is speculated that hypoxia induced increased autophagy to eliminate dysfunctional mitochondria, maintained the stability of ROS and MMP, and did not trigger apoptosis.

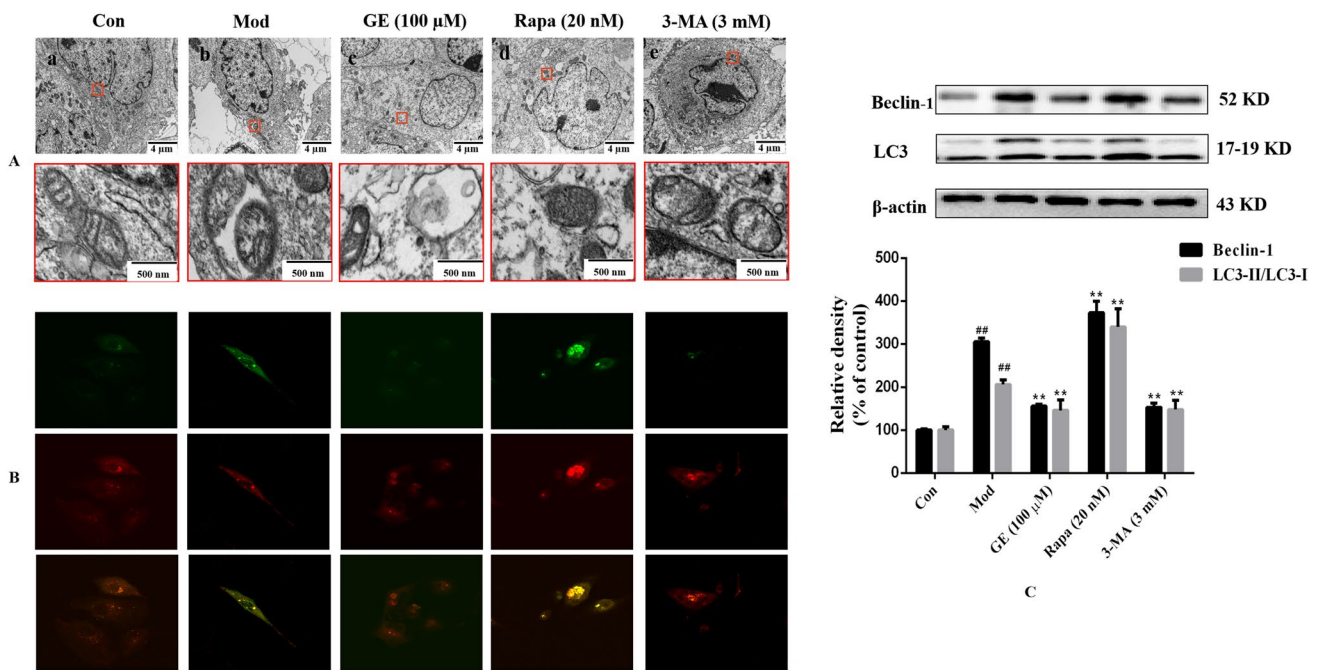


**Fig. 7** Effects of GE on the autophagy of FLSs. **A** After exposed to GE for 24 h, cells were analyzed by electron microscopy. **B** FLSs were infected with EGFP-LC3 (Green) for 24 h and then treated with GE, mitochondria were marked with Mitotracker (Red). **C** The expression of Beclin-1 and LC3 was analyzed by Western blot. Val-

ues were expressed as the mean  $\pm$  SD. Statistical analysis were shown three independent replicates. <sup>#</sup> $P < 0.05$ , <sup>##</sup> $P < 0.01$  compared with control group; \* $P < 0.05$ , \*\* $P < 0.01$  compared with model group (color figure online)

GE (100  $\mu$ M) inhibited autophagy, induced the accumulation of ROS and the decrease of MMP, and triggered apoptosis, which was an important factor for GE to reduce the proliferation of FLSs.

### GE blocked JNK-BNIP3 pathway to suppress autophagy in FLSs

The difference in autophagy ability is closely related to the expression of BNIP3 [11]. Since HIF-1 $\alpha$  is a core transcription factor under hypoxia and an upstream molecule that regulates the transcriptional activity of BNIP3, the expression of HIF-1 $\alpha$  under different hypoxia times was first detected. The mRNA and protein of HIF-1 $\alpha$  were low under 21% O<sub>2</sub>, and the mRNA expression of HIF-1 $\alpha$  increased slightly with the increase of hypoxia time, while the protein expression of HIF-1 $\alpha$  was largely accumulated. In HIF-1 $\alpha$  target gene, the expression of BNIP3 was further detected. A small amount of BNIP3 was expressed under 21% O<sub>2</sub>. With the extension of hypoxia time, the mRNA and protein expression of BNIP3 enhanced at 2% O<sub>2</sub>. In addition, multiple bands of BNIP3 appeared at 30 kDa (Fig. 10A, B).

To determine the mechanism by which GE suppressed autophagy, we investigated the regulatory effect of GE on the key inducer of autophagy, BNIP3. GE (100  $\mu$ M) and

3-MA (3 mM) reduced the protein expression of BNIP3, and the signal of the band originally located at 30 kDa was inhibited. Rapa (20 nM) further led to the accumulation of HIF-1 $\alpha$  and BNIP3 (Fig. 10C). The mRNA expressions of HIF-1 $\alpha$  and BNIP3 had no significant change after GE, 3-MA, and Rapa treatment (Fig. 10D). As shown by RT-qPCR results, GE did not decrease the mRNA expressions of HIF-1 $\alpha$  and BNIP3, but repressed their protein expressions, which was contradictory. Previous experiments have confirmed that GE promoted the degradation of HIF-1 $\alpha$  by activating the prolyl hydroxylase-von Hippel-Lindau pathway [20]. In addition, studies have confirmed that BNIP3 is a rapid degradation protein [21].

Hypoxia enhanced the activation of the JNK pathway in FLSs [22]. Our results re-confirmed that JNK pathway was overactivated under 2% O<sub>2</sub>, and the p-JNK/JNK ratio was significantly increased, while GE (100  $\mu$ M) down-regulated the p-JNK/JNK ratio as in previous results (Dai et al., 2014) (Fig. 10E). Autophagy was activated through JNK-BNIP3 pathway [23, 24]. To further verify the direct effect of p-JNK and BNIP3, a co-immunoprecipitation assay was used to detect the co-expression of p-JNK and BNIP3. Under 2% O<sub>2</sub>, p-JNK and BNIP3 were co-expressed and were decreased under GE (100  $\mu$ M) and 3-MA (3 mM). Rapa (20 nM) further up-regulated the co-expression of p-JNK and BNIP3 (Fig. 10F). GE lowered

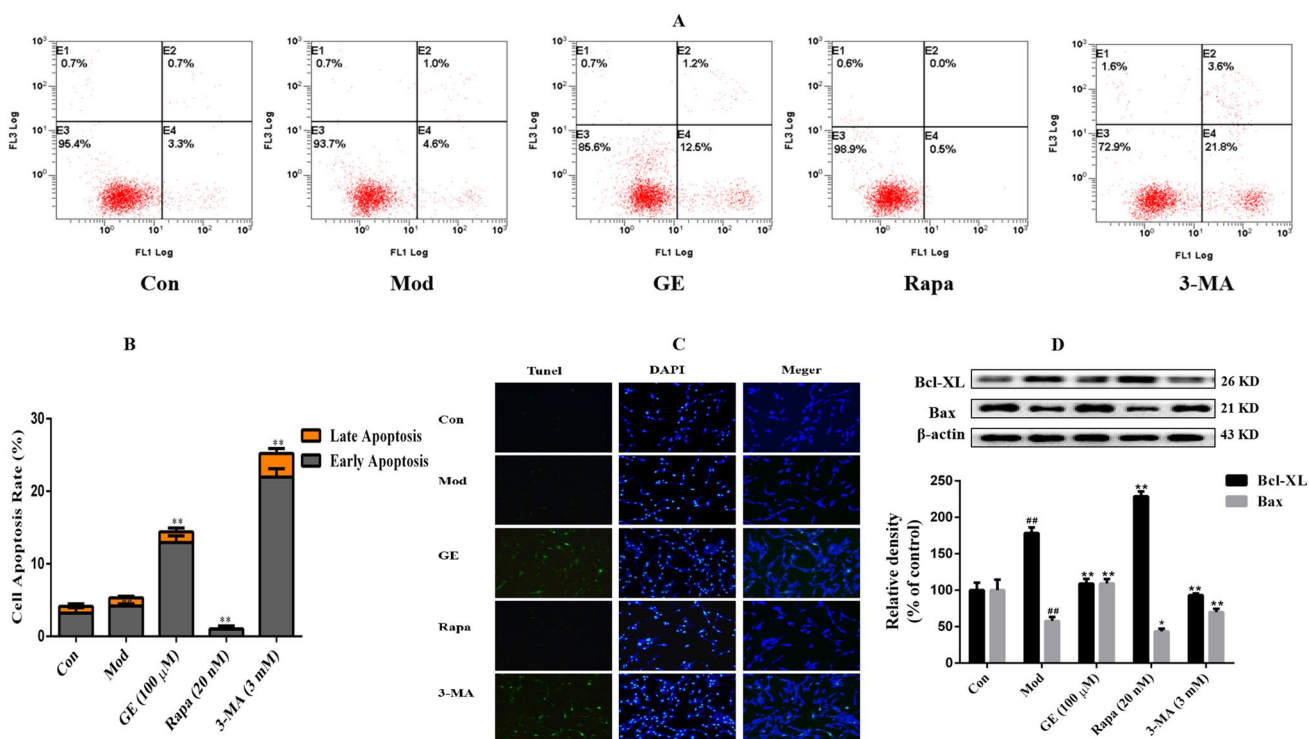


**Fig. 8** Effects of GE on the apoptosis of FLSs. **A** After exposed to GE for 24 h, FLSs were analyzed by FCM using Annexin V/PI double-staining; **B** histogram depicts the quantitative data from the AV/PI double staining; **C** representative fluorescence images of FLSs stained with TUNEL and Propidium Iodide to visualize apopto-

sis cells (Green) and nucleus (Blue); **D** the expressions of Bax and Bcl-XL were analyzed by Western blot. Values were expressed as the mean ± SD. Statistical analysis were shown three independent replicates. #*P* < 0.05, ##*P* < 0.01 compared with control group; \**P* < 0.05, \*\**P* < 0.01 compared with model group (color figure online)

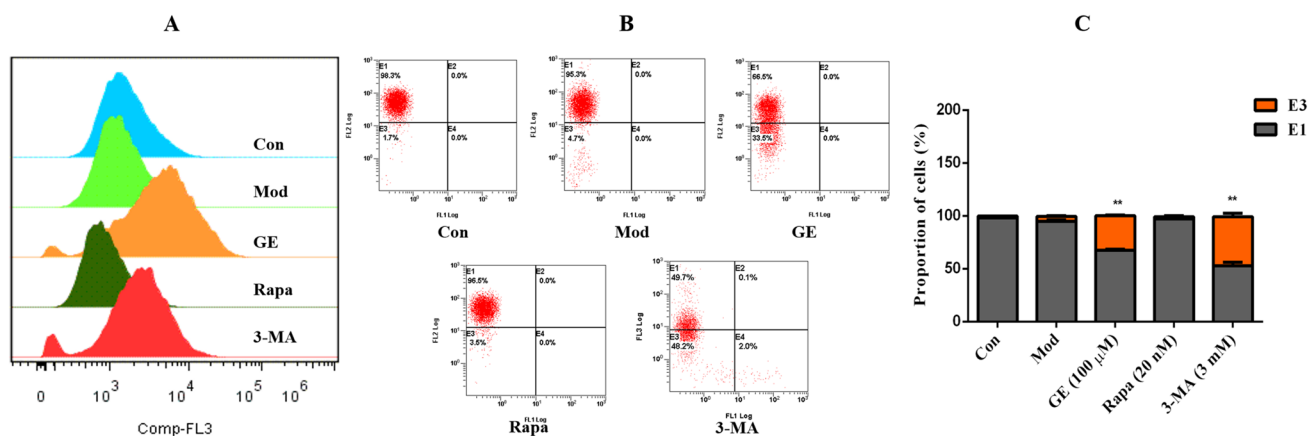


**Fig. 9** Effect of GE on oxidation indexes in FLSs. **A** FLSs were exposed to GE for 24 h and assessed the ROS content by FCM using 10 μM CM-H2DCFDA; **B** JC-1 was used to detect the effect of hypoxia on MMP of FLSs. **C**

Histogram depicts the quantitative data from the JC-1 staining. Values were expressed as the mean ± SD. Statistical analysis were shown three independent replicates. #*P* < 0.05, ##*P* < 0.01 compared with control group; \**P* < 0.05, \*\**P* < 0.01 compared with model group

the abnormal phosphorylation of JNK induced by hypoxia and decreased the co-expression of p-JNK and BNIP3, but had no effect on the mRNA expression of HIF-1α and BNIP3 (see Fig. 11).

### Discussion

The abnormal proliferation of FLSs is the main factor leading to hyperplasia of synovium in RA, which is

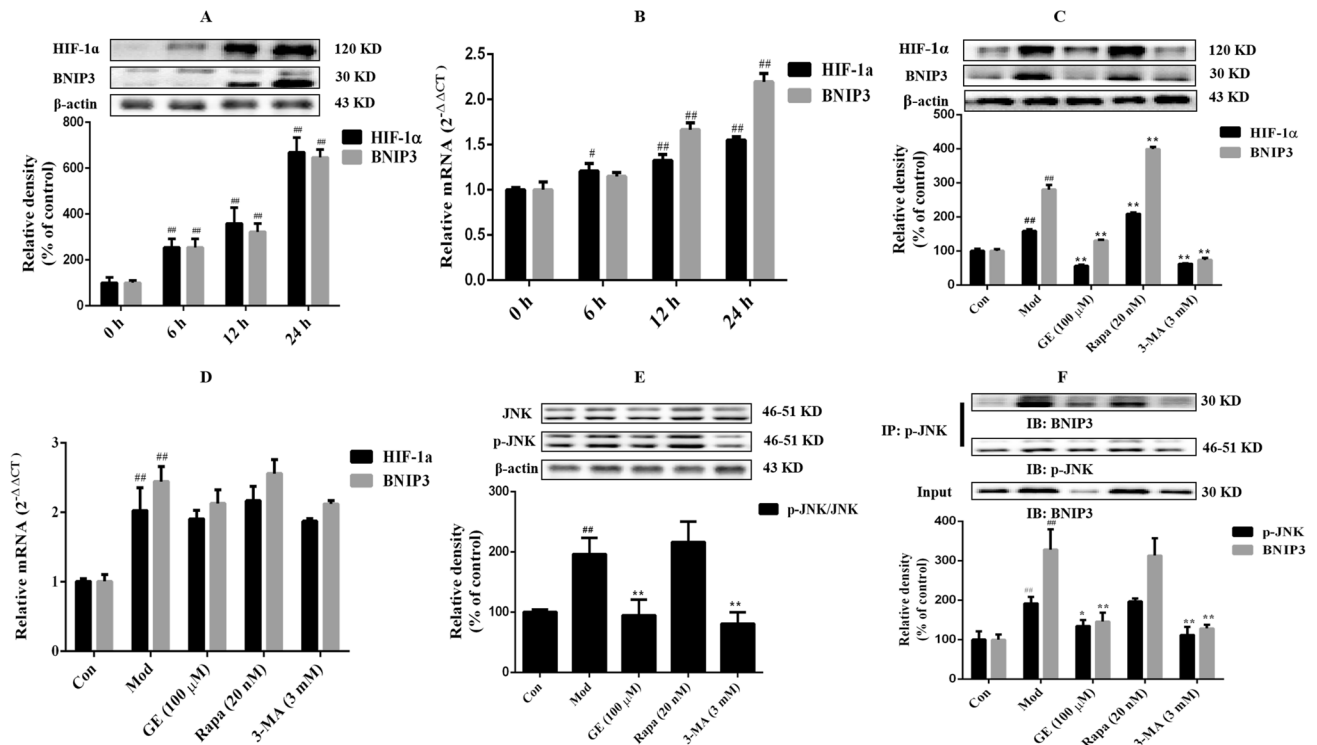


**Fig. 10** GE lowered the overactivated JNK-BNIP3 pathway to reduce autophagy in FLSs. **A** Protein expressions of HIF-1 $\alpha$  and BNIP3 in FLSs at different hypoxia times; **B** the mRNA expressions of HIF-1 $\alpha$  and BNIP3 in FLSs at different hypoxia times; **C** effect of GE on the expressions of HIF-1 $\alpha$  and BNIP3 in FLSs; **D** effect of GE on the mRNA expressions of HIF-1 $\alpha$  and BNIP3 in FLSs; **E** effect of GE

on the ratio of p-JNK/JNK in FLSs; **F**: Co-expression of p-JNK and BNIP3 in FLSs by immunoprecipitation and the intervention of GE. Values were expressed as the mean  $\pm$  SD. Statistical analysis were shown three independent replicates. # $P$  < 0.05, ## $P$  < 0.01 compared with control group; \* $P$  < 0.05, \*\* $P$  < 0.01 compared with model group

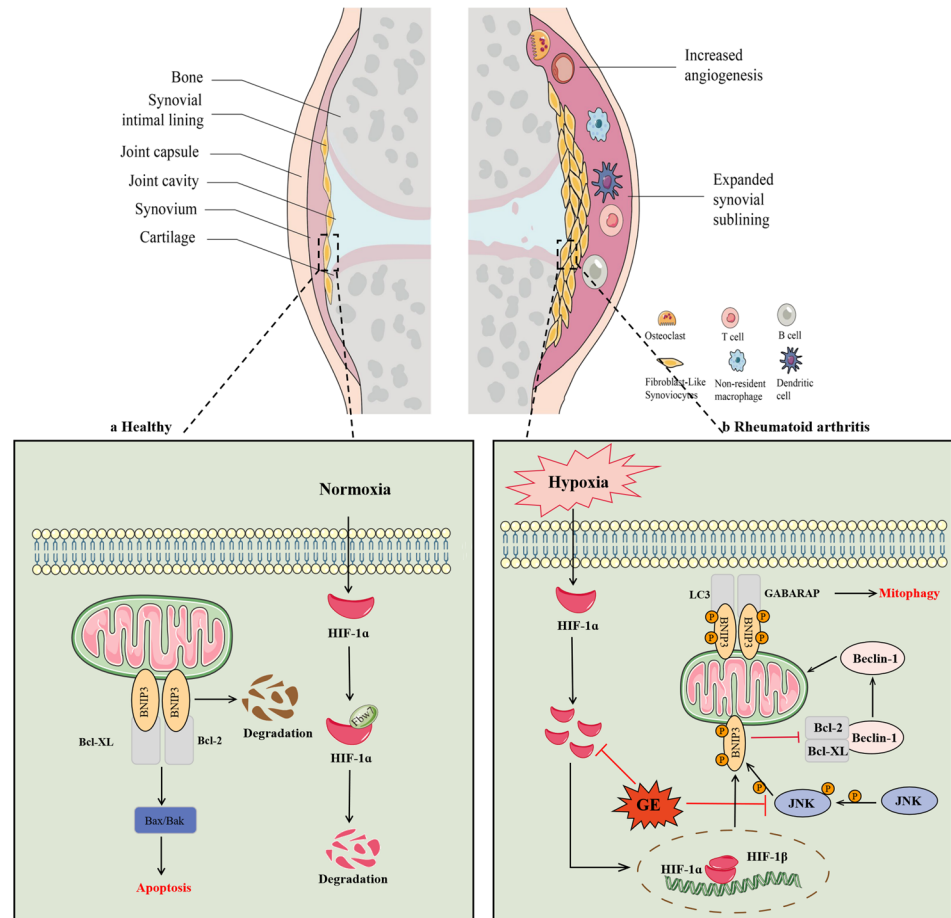
accompanied by dynamic changes in autophagy and apoptosis and has been the focus of attention [25]. Interestingly, the complex relationship between autophagy and apoptosis appears to vary from disease to disease. This study aimed to clarify the dynamic changes of autophagy and apoptosis in RA and the role of autophagy in hyperplasia dysplasia. The difference in the redox state of FLSs at different oxygen concentrations seems to have a great influence on its survival. Under the condition of 2% O<sub>2</sub>, the contents of ROS and MMP in FLSs remained relatively stable, the apoptosis did not change significantly, and the proliferation of FLSs was enhanced. At 0.5% O<sub>2</sub>, the proportion of FLSs accompanied by ROS accumulation and MMP reduction increased, while apoptosis was triggered in large numbers. The increase in apoptosis caused by the imbalance of redox may be an important factor in the decrease in the survival rate of FLSs under 0.5% O<sub>2</sub> [26].

Is the difference in FLSs survival mediated by autophagy at 21%, 2%, and 0.5% O<sub>2</sub>? The results showed that 2% O<sub>2</sub> promoted the occurrence of autophagy, which confirmed that autophagy was one of the protective mechanisms for promoting cell survival under hypoxia, consistent with the previous research results [27, 28]. Autophagy increased at

0.5% O<sub>2</sub>, but significantly less than that at 2% O<sub>2</sub>. The variation of autophagy under different oxygen concentrations may be related to the different activation signal pathways, which lead to the change in the survival of cells. Some studies have confirmed that hypoxia induced apoptosis and reduced cell viability [29]. It has been hypothesized that the paradoxical effects of hypoxia on autophagy and apoptosis may be due to differences in hypoxia concentrations or the type of disease. As we observed, 2% O<sub>2</sub> induced a significant increase in autophagy, while autophagy decreased, and apoptosis increased when oxygen concentration was less than 1%.

To further confirm that autophagy is a major factor mediating the survival difference of cells under different oxygen concentrations, we examined the effect of autophagy inhibitor 3-MA on FLSs survival indicators. 3-MA is a classical autophagy inhibitor, which plays an inhibitory role in the formation and development of autophagosomes. In the synovium of AA rats, 3-MA (15 mg/kg) alleviated abnormal synovium hyperplasia and inflammatory infiltration by suppressing autophagy to induce apoptosis. After 3-MA (3 mM) restrained autophagy of FLSs, the accumulation of ROS enhanced, and the apoptosis heightened accompanied by a decrease in survival rate under the condition of 2%

**Fig. 11** The synovial joint in health and in RA. **A** In healthy joints, the lining tissue of synovial intima is loose, with only one or two layers of FLSs. HIF-1 $\alpha$  cannot accumulate in normal synovium, BNIP3 binds to Bcl-2 and Bcl-XL, while Bax and Bak play a pro-apoptotic effect and induce the normal death of FLSs. **B** In RA, the synovial lining of the joint is greatly expanded; FLSs proliferate abnormally and further progress to invasive pannus. In the hypoxic microenvironment, a large amount of HIF-1 $\alpha$  accumulates and merges into the nucleus, activates the expression of BNIP3, and inhibits the Bcl-2/Bcl-XL/Beclin-1 complex to release Beclin-1. BNIP3 further combined with LC3 to promote autophagy, resulting in reduced apoptosis and enhanced proliferation of FLSs



$O_2$ , which confirmed that autophagy enhanced cell viability at 2%  $O_2$  by clearing ROS and reducing MMP. Under 0.5%  $O_2$ , while suppression of autophagy resulted in a slight augment in ROS accumulation, the proportion of FLSs in MMP declined, and apoptosis rate increased slightly, while decreasing the cell viability. A small amount of autophagy at 0.5%  $O_2$  was not enough to eliminate the excessive accumulation of ROS and decreased MMP, and oxidative stress triggered apoptosis. These results confirmed that activation of autophagy exacerbated synovial hyperplasia and hypoxia in AA rats by inhibiting apoptosis, suggesting that inhibition of high levels of autophagy in FLSs may be a potential target for RA treatment [30].

BNIP3 is a hypoxia-inducible BH3-only member of the Bcl-2 family of proteins that regulates apoptosis and autophagy. Previous studies have confirmed that the characteristics of abnormal proliferation and insufficient apoptosis of FLSs under the condition of hypoxia were closely related to BNIP3-mediated autophagy. Silencing of BNIP3 reduced the amount of autophagy and enhanced the apoptosis rate, suggesting that BNIP3 played an active role in the adaptive response of FLSs under the condition of hypoxia [11]. Our results confirmed that GE inhibited hypoxia-induced

excessive proliferation and autophagy and promoted apoptosis in FLSs, which may be related to the JNK-BNIP3 signaling pathway. It was confirmed that ROS accumulated in hypoxia triggered the activation of JNK. In turn, activated JNK mediated BNIP3-induced autophagy activation [31]. Furthermore, studies have confirmed that JNK is involved in the regulation of BNIP3 phosphorylation to mediate the change of BNIP3 protein expression and activate the occurrence of autophagy under hypoxia, which suggested that hypoxia has a good mechanism for the regulation of JNK activity [32]. JNK is expected to become a potential therapeutic target for RA. Our group confirmed that GE reduced the activation of FLSs on vascular endothelial cells through targeted inhibition of sphingosine kinase 1 (SphK1) pathway [33]. Studies have demonstrated that SphK1 interacted with JNK, and silencing of SphK1 inhibited the phosphorylation of JNK and mitochondrial permeability transition [34, 35]. The regulatory effect of GE on BNIP3-mediated autophagy may be related to its targeted inhibition of the transmembrane of SphK1, thereby down-regulating the overactivation of JNK. While other studies have shown that JNK mediated the upregulation of SphK1

[36]. The specific regulatory mechanism of GE on BNIP3 and its mediated autophagy needs to be further studied.

Multiple proteins in the Bcl-2 family that regulate cell death have complex regulatory mechanisms, including phosphorylation and ubiquitin modification at the protein level and shearing modification at the RNA level, which result in changes in their functions [37, 38]. This is also the reason why pro-apoptotic proteins in the Bcl-2 family are highly expressed in tumors. These studies suggested that BNIP3, a member of the Bcl-2 family, may also have a post-transcriptional regulatory role. 30 kDa band has always been regarded as the standard band for judging BNIP3. We found that BNIP3 showed multiple bands under hypoxia and speculated that it might have undergone post-transcriptional modification. It has been reported that the phosphorylation of BNIP3 increased the stability of BNIP3, which was the key factor affecting the appearance of different migration bands of BNIP3 in SDS-PAGE electrophoresis [39]. However, whether the phosphorylation modification of BNIP3 is related to the Dwifungsi function of promoting cell survival or death is the question we need to verify in the next step.

In conclusion, GE played a therapeutic role in RA by lowering the overactivated JNK-BNIP3 signaling pathway and its mediated autophagy, leading to the accumulation of ROS and the decrease of MMP, as well as an increase in apoptosis. The post-translational modification process of BNIP3 may be involved in this process.

**Acknowledgements** This work was supported by the National Natural Science Foundation of China (No 81874360, No 81473400, and No 81073122), the Major Natural Science Research Projects of Anhui Province Colleges and Universities (KJ2021ZD0060), and the Natural Science Research Project of Anhui Educational Committee (2022AH050453).

**Author contributions** RD and HW contributed to the conception and design of the study. RD wrote the first draft of the manuscript. RD, YW, and YH B wrote sections of the manuscript. All authors contributed to the article and approved the submitted version.

**Data availability** All data generated during this study are included in this published article.

## Declarations

**Conflict of interest** The authors declare no competing interests.

## References

- Xiao C, Lv C, Sun S, Zhao H, Ling H, Li M, et al. TSP1 is the essential domain of SEMA5A involved in pannus formation in rheumatoid arthritis. *Rheumatology (Oxford)*. 2021;60(12):5833–42.
- Masoumi M, Bashiri H, Khorramdelazad H, Barzaman K, Hashemi N, Sereshki HA, et al. Destructive roles of fibroblast-like synoviocytes in chronic inflammation and joint damage in rheumatoid arthritis. *Inflammation*. 2021;44(2):466–79.
- Fang J, Chen Z, Lai X, Yin W, Guo Y, Zhang W, et al. Mesenchymal stem cells-derived HIF-1 $\alpha$ -overexpressed extracellular vesicles ameliorate hypoxia-induced pancreatic  $\beta$  cell apoptosis and senescence through activating YTHDF1-mediated protective autophagy. *Bioorg Chem*. 2022;129: 106194.
- Li J, Gong SH, He YL, Cao Y, Chen Y, Huang GH, et al. Autophagy is essential for neural stem cell proliferation promoted by hypoxia. *Stem Cells*. 2023;41: 77.
- Hou J, Gao W. IL-27 regulates autophagy in rheumatoid arthritis fibroblast-like synoviocytes via STAT3 signaling. *Immunobiology*. 2022;227(4): 152241.
- Vomero M, Caliste M, Barbati C, Speziali M, Celia AI, Ucci F, et al. Tofacitinib decreases autophagy of fibroblast-like synoviocytes from rheumatoid arthritis patients. *Front Pharmacol*. 2022;13: 852802.
- Yang J, Liu J, Li J, Jing M, Zhang L, Sun M, et al. Celastrol inhibits rheumatoid arthritis by inducing autophagy via inhibition of the PI3K/AKT/mTOR signaling pathway. *Int Immunopharmacol*. 2022;112: 109241.
- Vara-Pérez M, Rossi M, Van den Haute C, Maes H, Sassano ML, Venkataramani V, et al. BNIP3 promotes HIF-1 $\alpha$ -driven melanoma growth by curbing intracellular iron homeostasis. *EMBO J*. 2021;40(10): e106214.
- Chen BC, Weng YJ, Shibu MA, Han CK, Chen YS, Shen CY, et al. Estrogen and/or estrogen receptor  $\alpha$  inhibits BNIP3-induced apoptosis and autophagy in H9c2 cardiomyoblast cells. *Int J Mol Sci*. 2018;19(5):1298.
- Yao J, Wang J, Xu Y, Guo Q, Sun Y, Liu J, et al. CDK9 inhibition blocks the initiation of PINK1-PRKN-mediated mitophagy by regulating the SIRT1-FOXO3-BNIP3 axis and enhances the therapeutic effects involving mitochondrial dysfunction in hepatocellular carcinoma. *Autophagy*. 2022;18(8):1879–97.
- Deng R, Wang Y, Bu Y, Wu H. BNIP3 mediates the different adaptive responses of fibroblast-like synovial cells to hypoxia in patients with osteoarthritis and rheumatoid arthritis. *Mol Med*. 2022;28(1):64.
- Xiao Y, Ren Q, Zheng Y, Zhang S, Ouyang J, Jiao L, et al. Geniposide ameliorated dexamethasone-induced endoplasmic reticulum stress and mitochondrial apoptosis in osteoblasts. *J Ethnopharmacol*. 2022;291: 115154.
- Wang M, Wu H, Wang R, Dai X, Deng R, Wang Y, et al. Inhibition of sphingosine 1-phosphate (S1P) receptor 1/2/3 ameliorates biological dysfunction in rheumatoid arthritis fibroblast-like synoviocyte MH7A cells through G $\alpha$ i/G $\alpha$ s rebalancing. *Clin Exp Pharmacol Physiol*. 2021;48(8):1080–9.
- Wang RH, Dai XJ, Wu H, Wang MD, Deng R, Wang Y, et al. Anti-inflammatory effect of geniposide on regulating the functions of rheumatoid arthritis synovial fibroblasts via inhibiting sphingosine-1-phosphate receptors 1/3 coupling G $\alpha$ i/G $\alpha$ s conversion. *Front Pharmacol*. 2020;11: 584176.
- Dai MM, Wu H, Li H, Chen J, Chen JY, Hu SL, et al. Effects and mechanisms of Geniposide on rats with adjuvant arthritis. *Int Immunopharmacol*. 2014;20(1):46–53.
- Deng R, Bu Y, Li F, Wu H, Wang Y, Wei W. The interplay between fibroblast-like synovial and vascular endothelial cells leads to angiogenesis via the sphingosine-1-phosphate-induced RhoA-F-Actin and Ras-Erk1/2 pathways and the intervention of geniposide. *Phytother Res*. 2021;35(9):5305–17.
- Wang Y, Wu H, Gui BJ, Liu J, Rong GX, Deng R, et al. Geniposide alleviates VEGF-induced angiogenesis by inhibiting VEGFR2/PKC/ERK1/2-mediated SphK1 translocation. *Phytomedicine*. 2022;100: 154068.
- Laha D, Deb M, Das H. KLF2 (kruppel-like factor 2) regulates osteoclastogenesis by modulating autophagy. *Autophagy*. 2019;15(12):2063–75.

19. Touhami S, Béguier F, Yang T, Augustin S, Roubéix C, Blond F, et al. Hypoxia inhibits subretinal inflammation resolution thrombospondin-1 dependently. *Int J Mol Sci.* 2022;23(2):681.
20. Gan P, Sun M, Wu H, Ke J, Dong X, Chen F. A novel mechanism for inhibiting proliferation of rheumatoid arthritis fibroblast-like synoviocytes: geniposide suppresses HIF-1 $\alpha$  accumulation in the hypoxic microenvironment of synovium. *Inflamm Res.* 2022;71(10–11):1375–88.
21. Cizeau J, Ray R, Chen G, Gietz RD, Greenberg AH. The *C. elegans* orthologue ceBNIP3 interacts with CED-9 and CED-3 but kills through a BH3- and caspase-independent mechanism. *Oncogene.* 2000;19(48):5453–63.
22. Zhang Y, Zhou S, Cai W, Han G, Li J, Chen M, et al. Hypoxia/reoxygenation activates the JNK pathway and accelerates synovial senescence. *Mol Med Rep.* 2020;22(1):265–76.
23. Tsai CF, Yang SF, Lo CH, Chu HJ, Ueng KC. Role of the ROS-JNK signaling pathway in hypoxia-induced atrial fibrotic responses in HL-1 cardiomyocytes. *Int J Mol Sci.* 2021;22(6):3249.
24. Moberg M, Apró W, Horwath O, van Hall G, Blackwood SJ, Katz A. Acute normobaric hypoxia blunts contraction-mediated mTORC1- and JNK-signaling in human skeletal muscle. *Acta Physiol (Oxf).* 2022;234(2): e13771.
25. Barbati C, Colasanti T, Vomero M, Ceccarelli F, Celia AI, Pericone C, et al. Up-regulation of autophagy by etanercept treatment results in TNF-induced apoptosis reduction in EA.hy926 endothelial cell line. *Clin Exp Rheumatol.* 2021;39(3):606–11.
26. Asadollahi L, Mahoutforoush A, Dorreyatim SS, Soltanfam T, Paiva-Santos AC, Peixoto D, et al. Co-Delivery of erlotinib and resveratrol via nanostructured lipid Carriers: a synergistically promising approach for cell proliferation prevention and ROS-Mediated apoptosis activation. *Int J Pharm.* 2022;624: 122027.
27. He G, Nie JJ, Liu X, Ding Z, Luo P, Liu Y, et al. Zinc oxide nanoparticles inhibit osteosarcoma metastasis by downregulating  $\beta$ -catenin via HIF-1 $\alpha$ /BNIP3/LC3B-mediated mitophagy pathway. *Bioact Mater.* 2022;19:690–702.
28. Li Q, Liu Y, Huang Q, Yi X, Qin F, Zhong Z, et al. Hypoxia acclimation protects against heart failure postacute myocardial infarction via Fundc1-mediated mitophagy. *Oxid Med Cell Longev.* 2022;2022:8192552.
29. Zhang F, Luo H, Peng W, Wang L, Wang T, Xie Z, et al. Hypoxic condition induced H3K27me3 modification of the LncRNA Tmem235 promoter thus supporting apoptosis of BMSCs. *Apoptosis.* 2022;27(9–10):762–77.
30. Nam JH, Lee JH, Choi HJ, Choi SY, Noh KE, Jung NC, et al. TNF- $\alpha$  induces mitophagy in rheumatoid arthritis synovial fibroblasts, and mitophagy inhibition alleviates synovitis in collagen antibody-induced arthritis. *Int J Mol Sci.* 2022;23(10):5650.
31. Zhang J, Zhang C, Jiang X, Li L, Zhang D, Tang D, et al. Involvement of autophagy in hypoxia-BNIP3 signaling to promote epidermal keratinocyte migration. *Cell Death Dis.* 2019;10(3):234.
32. Jin Q, Li R, Hu N, Xin T, Zhu P, Hu S, et al. DUSP1 alleviates cardiac ischemia/reperfusion injury by suppressing the Mff-required mitochondrial fission and Bnip3-related mitophagy via the JNK pathways. *Redox Biol.* 2018;14:576–87.
33. Wang Y, Wu H, Deng R, Dai XJ, Bu YH, Sun MH, et al. Geniposide downregulates the VEGF/SphK1/S1P pathway and alleviates angiogenesis in rheumatoid arthritis in vivo and in vitro. *Phytother Res.* 2021;35(8):4347–62.
34. Di A, Kawamura T, Gao XP, Tang H, Berdyshev E, Vogel SM, et al. A novel function of sphingosine kinase 1 suppression of JNK activity in preventing inflammation and injury. *J Biol Chem.* 2010;285(21):15848–57.
35. Li L, Wang H, Zhang J, Sha Y, Wu F, Wen S, et al. SPHK1 deficiency protects mice from acetaminophen-induced ER stress and mitochondrial permeability transition. *Cell Death Differ.* 2020;27(6):1924–37.
36. Zhang W, Mottillo EP, Zhao J, Gartung A, VanHecke GC, Lee JF, et al. Adipocyte lipolysis-stimulated interleukin-6 production requires sphingosine kinase 1 activity. *J Biol Chem.* 2014;289(46):32178–85.
37. Wang Z, Song T, Guo Z, Cao K, Chen C, Feng Y, et al. Targeting the allosteric pathway that interconnects the core-functional scaffold and the distal phosphorylation sites for specific dephosphorylation of Bcl-2. *J Med Chem.* 2020;63(22):13733–44.
38. Bobo C, Céré C, Dufossée M, Dautant A, Moreau V, Manon S, et al. Improved electrophoretic separation to assist the monitoring of Bcl-xl post-translational modifications. *Int J Mol Sci.* 2019;20(22):5571.
39. Graham RM, Thompson JW, Wei J, Bishopric NH, Webster KA. Regulation of Bnip3 death pathways by calcium, phosphorylation, and hypoxia-reoxygenation. *Antioxid Redox Signal.* 2007;9(9):1309–15.

**Publisher's Note** Springer Nature remains neutral with regard to jurisdictional claims in published maps and institutional affiliations.

Springer Nature or its licensor (e.g. a society or other partner) holds exclusive rights to this article under a publishing agreement with the author(s) or other rightsholder(s); author self-archiving of the accepted manuscript version of this article is solely governed by the terms of such publishing agreement and applicable law.